THE ASTROPHYSICAL JOURNAL, 338:1033–1046, 1989 March 15

NON–LTE CO, REVISITED

THOMAS R. AYRES
Center for Astrophysics and Space Astronomy, University of Colorado
AND
GÜNTER R. WIEDEMANN
NASA Goddard Space Flight Center
Received 1988 May 31; accepted 1988 August 16

ABSTRACT

The fundamental ($\Delta v = 1$) vibration-rotation bands of carbon monoxide appear prominently in mid-infrared (2100 $cm^{-1} \approx 5$ μm) spectra of stars of solar temperature and cooler. The rapid pace of innovation in IR spectrometers and sensors, and controversial interpretations of exploratory CO spectra, have encouraged us to undertake a more extensive and detailed non–LTE simulation of the $\Delta v = 1$ bands than attempted previously. We formulated the equations of statistical equilibrium for a model molecule containing 10 bound vibrational levels, each split into 121 rotational substates and connected by more than 1000 radiative transitions. We solved for self-consistent populations and radiation fields by iterative application of the "Λ-operator" to an initial LTE distribution. We incorporated recent experimental measurements of the impact excitation of CO by atomic hydrogen, resolving the factor of 10^3 disagreement in CO-H cross sections used in earlier work.

We applied our non–LTE formalism to illustrative models of the Sun (G2 V) and the archetype red giant Arcturus (α Boo: K1 III). For the Sun we find negligible departures from LTE in either a theoretical radiative-equilibrium photosphere with outwardly falling temperatures in its highest layers or in a semiempirical hot chromosphere that reproduces the spatially averaged emission cores of Ca II H and K. While analogous models of Arcturus exhibit larger departures from LTE, the influence on synthesized spectra is comparatively minor. Non–LTE and LTE spectra are nearly identical for a semiempirical chromospheric model, but display small differences for a radiative equilibrium stratification. There the non–LTE "darkening" is a few percent in the residual fluxes of the strongest absorptions, equivalent to $\sim$200 K in the core brightness temperatures.

Our simulations demonstrate that the puzzling "cool cores" of the CO $\Delta v = 1$ bands observed in limb spectra of the Sun and in flux spectra of Arcturus cannot be explained simply by non–LTE scattering effects. Instead, they likely result from a bifurcation of the outer atmosphere into cool zones where the CO absorptions form and hot zones where the Ca II emissions arise.

Subject headings: infrared: spectra — line formation — molecular processes — radiative transfer — stars: abundances — stars: late-type

I. INTRODUCTION

The vibration-rotation bands of carbon monoxide are a valuable spectral thermometer for cool stellar atmospheres (Hall 1970). In recent years, there has been renewed interest in the infrared spectrum of CO owing to a puzzling series of observations of the 2100 cm^{-1} fundamental ($\Delta v = 1$) absorptions in the red giant Arcturus (α Boo: K1 III) and the Sun.

Heasley *et al.* (1978) discovered that the most opaque of the CO fundamental lines in Arcturus were purely in absorption, contrary to earlier predictions of chromospheric emission cores (Heasley and Milkey 1976). Ayres and Testerman (1981, hereafter AT) found a similar dichotomy in infrared spectra of the Sun: the depressed core brightness temperatures of strong $\Delta v = 1$ lines at the extreme limb (also noted by Noyes and Hall 1972) were inconsistent with the weak emission reversals predicted by chromospheric models.

The dark cores of the strong CO fundamental lines are thought to form in a highly inhomogeneous atmosphere. Much of the gas at "chromospheric" heights must be cool ($T \lesssim 4000$ K), while a lesser amount resides at truly chromospheric temperatures ($T \gtrsim 6000$ K; Ayres 1981): the classic emission reversals of resonance lines like Ca II H and K arise not in a uniform temperature inversion, but rather as a spatial average over a fragmented patchy array of small-scale bright points (e.g., Foing and Bonnet 1984; Ayres, Testerman, and Brault 1986, hereafter ATB).

More recently, Anderson (1989) has constructed a non–LTE line-blanketed radiative-equilibrium (RE) model of the solar atmosphere: it strongly supports the key role of CO surface cooling proposed earlier by Johnson (1973) in the context of the outer photospheres of late-type giants, and later by Ayres (1981) in the "thermal bifurcation" of the solar chromosphere.

However, the conclusions of the semiempirical modeling by AT and ATB, and the analytical arguments of Ayres (1981), must be tempered by the authors' use of the LTE assumption. For example, it is possible that non–LTE "core darkening" might mimic the appearance of a cool outer photosphere in the extreme-limb spectra recorded by AT. Further, the strong surface cooling by the CO bands in Anderson's RE model might be attributed, in part, to the superficial treatment of non–LTE effects driven by the global scope of the atomic and molecular simulation. Thus, a careful examination of the possible influence of non–LTE effects on the infrared bands of CO is warranted.

a) *Previous Studies of Non–LTE* CO

Thompson (1973) demonstrated semi-quantitatively that rotational LTE should obtain in virtually all stars of late spec-

tral type, and that the ionization and chemical equilibria of CO should be very near LTE as well. Nevertheless, the available collisional rates suggested that departures of the *vibrational* populations from the Boltzmann distributions could occur in the low-pressure atmospheres of cool giants.

Hinkle and Lambert (1975, hereafter HL) called attention to the critical role of CO-H collisions, and the serious factor of 10^3 difference between Thompson's rates based on a scaling formula of Millikan and White (1963, hereafter MW), and the experimental cross sections of von Rosenberg, Taylor, and Teare (1971, hereafter VTT).

Carbon, Milkey, and Heasley (1976, hereafter CMH) conducted the first quantitative study of statistical equilibrium and radiative transfer in CO. The authors' numerical simulations explored the general thermalization properties of the vibration-rotation bands and outlined a domain of atmospheric conditions where departures from LTE could be significant. Like HL, CMH confirmed the critical importance of CO-H collisions: the large—but controversial—cross sections reported by VTT prevented significant departures from LTE except in the most tenuous outer layers of the coolest red supergiants.

b) *Present Work*

A strong motivation for a reexamination of non–LTE effects in CO has been the introduction of cryogenically cooled spectral isolators for the large stellar Fourier transform spectrometers (e.g., Wiedemann *et al.* 1987). Infrared spectra from the new devices are sufficiently good to demand a treatment of the CO line-formation problem of comparable quality, in order to avoid misinterpretations arising from small, but systematic, deviations from LTE.

In the present paper we describe a simple strategy to solve the non–LTE problem for the $\Delta v = 1$ bands of CO; we review available experimental measurements of the impact excitation of CO by a variety of collision partners, including new results for CO-H; and we calculate synthetic spectra for illustrative models of the Sun and Arcturus to test the effects of departures from LTE in situations of practical interest.

II. METHOD

a) *Overview*

The non–LTE problem for a molecule like CO is formidable. One must incorporate at least the first 10 vibrational levels, and more than 100 rotational substates for each, merely to accommodate the thousands of transitions *observed* in the 1900–2200 cm^{-1} region of late-type stars. Each vibration-rotation line profile must be sampled finely enough in frequency to accurately represent the local radiation field. The model atmosphere must contain a sufficient number of layers to resolve the $\tau \approx 1$ zones for strong and weak CO transitions, and the photospheric continuum. Worse yet, the CO problem in the luminous red giants is really *two* problems, owing to the conspicuous $^{13}C^{16}O$ bands in the evolved isotopically enriched photospheres (CMH). The thousands of levels and transitions present severe difficulties for conventional non–LTE numerical solution techniques like the widely used LINEAR-A code of Auer, Heasley, and Milkey (1972). For example, CMH were forced to recast the partial linearization procedure in terms of the net radiative rates (following Auer and Heasley 1976), to achieve substantial economies in their 200 level model molecule compared with the standard formulation in terms of the frequency-dependent radiation fields.

b) *Solution by Lambda Iterations*

Solving the non–LTE problem in CO using the powerful techniques developed for atomic transitions, as CMH did, was a natural approach. However, the molecular problem differs in important ways from the more familiar situation of atomic resonance lines, permitting it to be solved using simpler numerical schemes: these in turn allow one to treat a model molecule in realistic detail.

Figure 1 illustrates the practical differences between the energy spectrum of CO and that of a typical simple ion. The molecule has a vast array of relatively low-lying states, connected to each other by an equally vast collection of weak infrared transitions. The ion has only a few low-lying levels, connected by only a few—but strong—optical transitions.

Owing to the small spontaneous emission rates for the $\Delta v = 1$ transitions ($A_{ul} \lesssim 2 \times 10^2$ s^{-1}), collisional de-excitations typically exceed radiative decays in the atmospheric layers where the most opaque CO lines form. Because the collisional quenching of CO is dominated by atomic hydrogen, the rates follow the exponential inward increase of n_H imposed by hydrostatic equilibrium. Even if $\epsilon \equiv C_{ul}/A_{ul} < 1$ near line-center optical depth unity, the rapid inward increase in density should enforce collisional LTE ($\epsilon \gg 1$) within a few optical depths of $\tau_{1c} = 1$.

In the atomic resonance-line problem, on the other hand, the fast spontaneous decay rate ($A_{ul} \approx 10^8$ s^{-1}) forces the collisional ϵ's to be small ($\approx 10^{-4}$) where the line core forms. Because the collisional quenching is dominated by electrons rather than atomic hydrogen (see discussion by HL), ϵ remains small throughout the entire stellar chromosphere, where n_e is roughly independent of height (e.g., Ayres 1979). Consequently, departures from LTE in atomic resonance lines tend to be substantial and LTE obtains only at large optical depths. It is for that difficult scattering-dominated problem that the powerful partial-linearization solution schemes were developed.

Because the CO bands are much closer to LTE, a simpler approach is feasible: the "Λ-iteration" (Mihalas 1978, § 6-1). In essence, one initially fixes the populations at their LTE values, then iterates between the formal solution of the radiative transfer problem (for specified populations) and the solution of the steady state rate equations (for specified radiation fields) until they are self-consistent. The procedure, in fact, is an integral part of the partial-linearization techniques: it is used to "smooth" the solutions between the major linearization cycles (e.g., Auer, Heasley, and Milkey 1972).

The principal drawback of the "Λ-operator" is that it propagates scattering information only an optical mean free path ($\Delta\tau \approx 1$) at a time (Mihalas 1978, p. 149). Thus, a prohibitive number of iterations would be required to converge a typical "long-range" atomic resonance line problem where the thermalization length ($\approx \epsilon^{-1}$) might be as large as 10^4 line-center optical depths. In the CO problem, on the other hand, the large value of ϵ where the line cores form, and its rapid inward increase, guarantee that LTE will be attained within a few optical depths of $\tau_{1c} = 1$: only a few Λ-iterations should converge the populations and radiation fields to self-consistency.

The principal attraction of the Λ-iteration is computational speed. Because the partial-linearization schemes must account explicitly for the coupling between the radiation transport and the statistical equilibrium, they can achieve timings no better

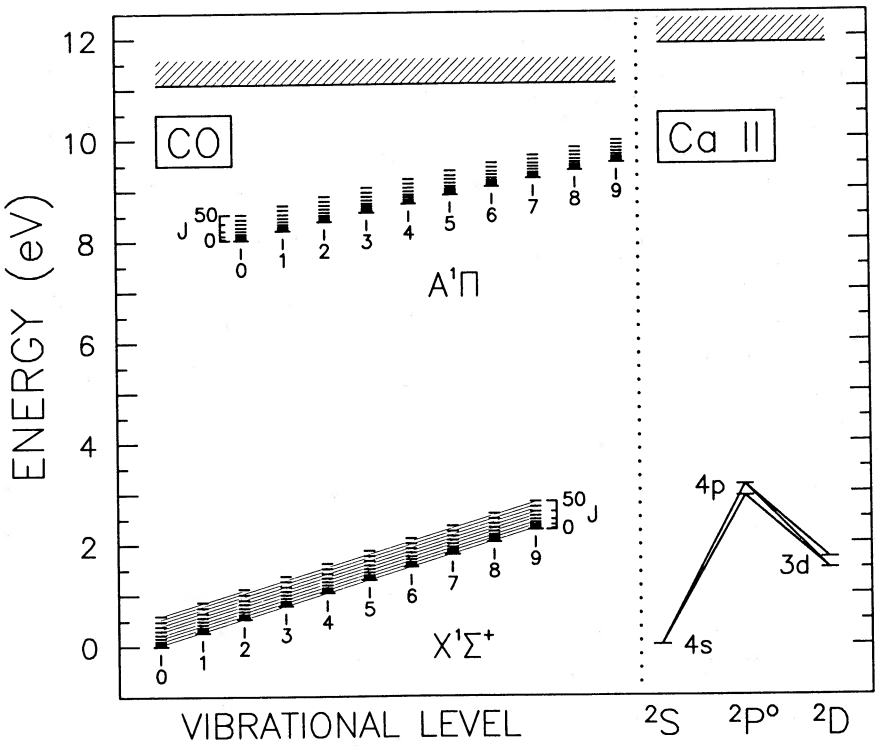

FIG. 1.—Schematic energy levels of CO and the astrophysically important ion Ca II. For CO the ground state and one of the excited electronic states are depicted. For Ca II the ground state and the lowest-lying excited states are illustrated (the transitions 4*s*–4*p* are the H and K resonance lines near 3950 Å). The hatched bars indicate the dissociation energy of CO and the ionization energy of Ca II: both species are relatively durable in cool stellar atmospheres. The electronic ground state of CO is split into a vast collection of vibration-rotation levels, connected by thousands of radiative transitions. The small energy separations ensure that the several lowest lying v levels are well populated in the cool layers of solar-type and later atmospheres. Because there are so many radiative channels the individual oscillator strengths are small: the $\Delta v = 1$ bands would be quite weak were it not for the large cosmic abundances of C and O. In the case of Ca II there are relatively few distinct levels connected by equally few radiative transitions. The substantial energy gaps ensure that most of the population in a cool gas will be concentrated in the ground state. This and the large oscillator strengths of the resonance doublet guarantee that the H and K features will be quite strong in the near-ultraviolet spectra of cool stars despite the small cosmic abundance of calcium ($\lesssim 1\%$ A_C).

than quadratic in the number of transitions (Mihalas 1978, § 12–3). In the Λ-iteration the two problems are solved separately and the timing is strictly linear in $N_{\rm trans}$: a distinct advantage when modeling the $\approx 10^3$ lines in the CO $\Delta v = 1$ bands. Furthermore, economies can be applied to the separate problems that would not be practical if they were solved jointly.

c) *The Model* CO *Molecule*

In what follows, double-primes refer to the lower level of a transition and single-primes refer to the upper level. Unprimed quantities appear where a transition is not involved or the level assignments are not ambiguous.

We treat a model molecule with $N_v = 10$ vibrational levels ($v = 0, \ldots, 9$), each split into $N_J = 121$ rotational states ($J = 0, \ldots, 120$). To simplify bookkeeping and to reduce the number of line transitions that must be simulated, we replace the R ($J' = J'' + 1$) and P ($J' = J'' - 1$) branches of the true fundamental bands with a fictitious "Q-branch" (with selection rule $J' = J''$) consisting of *pairs* of identical transitions from each rotational state.

We calculate absorption oscillator strengths as follows (Allen 1973, § 26):

$$f_{v''J''v'J'} = 1.499\omega_0^{-2}(g_{v'J'}/g_{v''J''})A_{v'J'v''J''}\,, \qquad (1)$$

where ω_0 is the wavenumber (cm^{-1}) of the line; the ratio of statistical weights is unity for the fictitious Q-branch; and $A_{v'J'v''J''}$ is the Einstein coefficient for the downward transition. We assume that the total $\Delta v = 1$ spontaneous decay rate for a rotational state is independent of J' (rotationless: see, e.g., Kurucz 1976) and equal to the experimental value for the vibrational band, $A_{v'v'-1}$. Because there are two identical transitions from each upper state J', the spontaneous decay rate for an individual Q-branch transition is

$$A_{v'J'v'-1J'} = \tfrac{1}{2}A_{v'v'-1}. \qquad (2)$$

We adopted the band A-values tabulated by Radzig and Smirnov (1985), which we reproduce in Table 1. The derived oscillator strengths are consistent with those of Kirby-Docken and Liu (1987) if one averages their values for the R- and P-branches (see Table 1). [Inexplicably, CMH adopted a constant log $gf = -6.70$ for their demonstration calculations: less than 10^{-3} of the true values for strong $\Delta v = 1$ lines. In reality, f itself is independent of J'', not $gf = (2J'' + 1)f_{v''J''}$.]

We enumerate the energy spectrum of the $X^1\Sigma^+$ electronic ground state according to that of a pure harmonic oscillator and pure rigid rotor:

$$E_{vJ} = \omega_0 v + B_0 J(J + 1)\,, \qquad (3)$$

where $\omega_0 = 2103$ cm^{-1} and $B_0 = 1.8951$ cm^{-1} closely reproduce the empirical term values of Mantz *et al.* (1975, as cited by Kurucz 1976) for the heavily populated levels ($v \leq 4$, $J \leq 50$). With the simplified energy spectrum the relative population of a vibration-rotation state in LTE is

$$n^*_{vJ} \sim \exp(-\beta v)\,(2J + 1)\exp[-\gamma J(J + 1)]\,, \qquad (4)$$

TABLE 1

SPONTANEOUS DECAY RATES AND *f*-VALUES

v_u (1)	A_{ul} (s^{-1}) (2)	f^Q_{lu} (10^{-5}) (3)	$\frac{1}{2}\langle f^R + f^P \rangle$ (10^{-5}) (4)
1.....	33	0.6	0.5
2.....	56	1.1	1.0
3.....	93	1.6	1.5
4.....	120	2.0	1.9
5.....	140	2.4	2.4
6.....	160	2.7	2.8
7.....	180	3.0	3.2
8.....	200	3.4	2.6
9.....	210	3.6	4.0

[a] Reference for Einstein coefficients (col. [2]): Radzig and Smirnov 1985.

[b] The oscillator strengths in col. (3) are for the fictitious "*Q*-branch" transitions that simulate the *R* and *P* branches of the true molecule.

[c] The oscillator strengths in col. (4) are averages of *R*- and *P*-branch values from the work of Kirby-Docken and Liu (1978; $J \gtrsim 10$).

where $\beta \equiv 1.43883\omega_0/T$ and $\gamma \equiv 1.43883B_0/T$, and T is the kinetic temperature. The strong collisional coupling among the rotational quantum states, and their extremely small Einstein *A*-values, should force them into a Boltzmann distribution at the local temperature (Thompson 1973). Thus, the population of any vibration-rotation state is simply $n_v \Psi_J$ (e.g., CMH), where n_v is the total population of level v and,

$$\Psi_J \equiv (2J+1)\exp\left[-\gamma J(J+1)\right] \Big/ \sum_{j=0}^{N_J-1} \times (2j+1)\exp\left[-\gamma j(j+1)\right] . \quad (5)$$

If we assume that radiation and collisions connect the levels only through $\Delta v = \pm 1$ transitions, the N_v steady state rate equations at each depth degenerate into $N_v - 1$ coupled "two-level-atom" relations:

$$n_v(R_{vv+1} + C_{vv+1}) - n_{v+1}(R_{v+1v} + C_{v+1v}) = 0 , \quad (6)$$

for $v = 0, \ldots, N_v - 2$. The R_{KK*} and C_{KK*} are radiative and collisional rates, respectively, connecting initial state K and final state $K*$. We replace the redundant N_v-th rate equation with number conservation,

$$\sum_{v=0}^{N_v-1} n_v = n_{\rm CO} . \quad (7)$$

In terms of departure coefficients, $b_v \equiv n_v/n_v{}^*$, the solution to the system of rate equations, closed by number conservation, is

$$b_v = \left[\sum_{V=0}^{N_v-1} \exp(-\beta V)\right]\left[\prod_{K=0}^{v} \Theta_K\right] \Big/ \sum_{V=0}^{N_v-1} \times \left[\exp(-\beta V)\prod_{K=0}^{V} \Theta_K\right], \quad (8)$$

where $\Theta_0 \equiv 1$ and,

$$\Theta_v \equiv \frac{b_v}{b_{v-1}} = e^{\beta}\frac{(R_{v-1v} + C_{v-1v})}{(R_{vv-1} + C_{vv-1})}, \quad (9)$$

for $v = 1, \ldots, N_v - 1$.

The Θ's can be evaluated as follows. The rotationless assumption permits us to write the radiative and collisional rates as band-averages over the rotational states. The radiative excitation rate is $R_{v-1v} = B_{v-1v}2\mathscr{J}_v$: B is the Einstein absorption coefficient; the factor of 2 accounts for the *pair* of transitions in the fictitious *Q*-branch; and $\mathscr{J}_v \equiv \sum_J \Psi_J \bar{J}_J$, where $\bar{J}_J = \int \phi_\omega J_\omega d\omega$ is the profile-weighted mean intensity of the Jth rotational transition of the $v' = v$ band. The radiative de-excitation rate is $R_{vv-1} = (A_{vv-1} + B_{vv-1}2\mathscr{J}_v)$: A is the Einstein coefficient for spontaneous decays; B is the Einstein coefficient for stimulted emissions; and again the factor of 2 accounts for the pair of *Q*-branch transitions. With $g_v/g_{v-1} \equiv 1$, the following relationships hold between the Einstein coefficients: $B_{v-1v} = B_{vv-1}$ and $B_{vv-1} = \frac{1}{2}A_{vv-1}/c_1$, where the $\frac{1}{2}$ is the branching ratio (eq. [2]) and $c_1 \equiv 2hc^2\omega_0{}^3$. Noting that the collisional excitation and de-excitation rates are connected by detailed balance,

$$C_{v-1v} = (n_v{}^*/n_{v-1}{}^*)C_{vv-1} = e^{-\beta}C_{vv-1} , \quad (10)$$

we can rewrite (e.g., Anderson 1989) the relation for Θ_v:

$$\Theta_v = \frac{(\mathscr{J}_v/\mathscr{B} + \mathscr{J}_v/c_1 + \epsilon_v)}{(1 + \mathscr{J}_v/c_1 + \epsilon_v)} , \quad (11)$$

where $\mathscr{B} \equiv c_1/(e^\beta - 1)$ is the Planck function and $\epsilon_v \equiv C_{vv-1}/A_{vv-1}$. Notice that LTE (i.e., $b_v \equiv 1\,\forall\, v$) is recovered in the important limits of (1) large collisional rates ($\epsilon \gg 1$); and (2) thermalization of the radiation fields ($\mathscr{J} \to \mathscr{B}$), regardless of the collisional rates.

In order to evaluate the individual $\bar{J}_J$'s that collectively determine each $\mathscr{J}_v$, we require absorption coefficients, κ_ω, and source functions, $\mathscr{S}_\omega$.

The monochromatic opacity is composed of contributions from the background continuum and the line (ignoring blending):

$$\kappa_\omega = \kappa_C + (\kappa_{vJ})_\omega . \quad (12)$$

In stars of solar type and later, the important continuous absorbers at 2100 cm^{-1} are free-free transitions in H^- and atomic hydrogen: we use the opacity formulae cited by Vernazza, Avrett, and Loeser (1976, 1981). The line contribution ($cm^2\ g^{-1}$) is (note: $v' = v$):

$$(\kappa_{vJ})_\omega = \frac{\pi e^2}{mc^2} f_{v-1v}\left(\frac{n_{v-1}}{\rho}\right)\left[1 - \left(\frac{b_v}{b_{v-1}}\right)e^{-\beta}\right]\phi_\omega , \quad (13)$$

where ρ is the material density ($g\ cm^{-3}$). We assume a Doppler line shape,

$$\phi_\omega = \frac{\exp\left\{-[(\omega - \omega_0)/\Delta\omega_{\rm D}]^2\right\}}{\sqrt{\pi}\,\Delta\omega_{\rm D}} , \quad (14)$$

with a depth-independent Doppler width $\Delta\omega_{\rm D}$ (cm^{-1}).

The monochromatic source function is

$$\mathscr{S}_\omega = (\kappa_C/\kappa_\omega)\mathscr{S}_C + (\kappa_{vJ}/\kappa_\omega)\mathscr{S}_{vJ} . \quad (15)$$

Conveniently, the source functions for $H_{\rm ff}{}^-$ and $H_{\rm ff}$ are the Planck function ($\mathscr{S}_C \equiv \mathscr{B}$). The line contribution, with complete frequency redistribution, is

$$\mathscr{S}_{vJ} = c_1/[(b_{v-1}/b_v)e^\beta - 1] . \quad (16)$$

d) Numerical Solution Scheme

While it would be straightforward to calculate the depth-dependent $\bar{J}_J$'s for each of the 121 unique *Q*-branch transitions of each of the nine possible vibrational bands, the smooth behavior of the rotational line opacity with J renders the com-

plete calculation unnecessary. For economy, we synthesized in detail only a subset of 11 representative rotational transitions in each vibrational band and interpolated over J with cubic splines to determine the complete set of $\bar{J}_J$'s at each depth.

We represented the discrete quadrature for $\bar{J}$,

$$\int_0^\infty \phi_\omega J_\omega d\omega \rightarrow \sum_{i=0}^{N_\omega - 1} \Phi_i J_i , \qquad (17)$$

by a mesh of N_ω = six frequency points distributed over the interval 0–2$\Delta\omega_D$ in the half-profile. We calculated the depth-dependent monochromatic mean intensities using Auer's (1976) Hermitian method with a grid of three direction cosines for the angular quadratures.

We began a computational cycle with LTE populations and iterated between the statistical equilibrium and the line formation until the maximum fractional change in the departure coefficients was less than 10^{-3} and decreasing consistently with each iteration. No more than five Λ-iterations were required for the lowest density models we considered.

e) *Collisional Rates*

The pioneering non–LTE CO studies by HL and CMH were diminished in their impact by the apparent factor of $\approx 10^3$ disagreement between the available cross sections for $\Delta v = 1$ collisional excitation of CO by atomic hydrogen: significant departures from LTE were found for the smaller cross sections, but essentially none for the larger. Thus, we have searched for more definitive measurements of CO collisional rates than were available previously.

Following Thompson (1973), we parameterize the collisional *de-excitation* rates in terms of the Landau-Teller formula:

$$\ln (P_X t_{CO\text{-}X}) = A_X T^{-1/3} - B_X , \qquad (18)$$

where P_X (atm) is the partial pressure of the collision partner "X"; $t_{CO\text{-}X}$ (s) is the relaxation time of the excited state of CO; and A_X and B_X are perturber-specific constants. Most of the existing CO-X experiments have been performed at low temperatures ($T < 3000$ K) and are sensitive primarily to the 1–0 fundamental transition. The associated collisional de-excitation rate is (Thompson 1973; HL):

$$C_{ul} = [t_{CO\text{-}X}(1 - e^{-\beta})]^{-1} . \qquad (19)$$

It is customary to write C_{ul} as a product of the density of perturbers, n_X (cm^{-3}), and a temperature-dependent factor, Ω_{ul} (cm^3 s^{-1}). In terms of the Landau-Teller constants and the excitation parameter β,

$$\Omega_{ul} = 4.2 \times 10^{-19} \frac{\exp [B_X - 0.069 A_X \beta^{1/3}]}{\beta(1 - e^{-\beta})} . \qquad (20)$$

Figure 2 compares CO $\Delta v = 1$ relaxation times for a variety of collision partners, including electrons. Table 2 lists the Landau-Teller parameters we adopted for CO-H, CO-H_2, and CO-He. In the Appendix we discuss our choices for the atom/diatom cross sections and CO-e^-.

f) *Model Atmospheres*

We specify a model by the stratification of temperature, T (K), with column mass density, m (g cm^{-2}), in discrete plane-parallel layers. Given the temperature profile, we solve the equations of hydrostatic equilibrium, chemical equilibrium, and ionization equilibrium jointly by means of a Newton-Raphson iteration scheme. We include turbulent pressure support as recommended by Vernazza, Avrett, and Loeser (1973, hereafter VAL). We allow for the LTE formation of H^-, H_2^+, and diatomic molecules of cosmically abundant elements. We adopt the molecular formation parameters of Kurucz (1970) and the solar abundances of VAL. We treat departures from LTE in hydrogen, but in a simple parametric way (see ATB).

TABLE 2

CO-X LANDAU-TELLER PARAMETERS

X[a]	A[b]	B[b]	Reference
H	3 ± 2	18.1 ± 0.2	1
H	(53)	(19.2)	2
H_2	64	19.1	1
H_2	(62)	(19.0)	3
He	87	19.1	4

[a] "X" is the collision partner for CO.

[b] The Landau-Teller coefficients A and B (eq. [18]) parameterize the relaxation time for collisional quenching of the 1–0 transition. Adopted values are listed first; previous results are listed in parentheses.

REFERENCES.—(1) Glass and Kironde 1982. (2) Millikan and White 1963. (3) Hooker and Millikan 1963. (4) Millikan 1964.

We focus on illustrative models of the Sun and the red giant Arcturus representing quite different regimes of effective temperature and gravity. We consider a pair of models for each star spanning the likely domains of temperatures and densities experienced by CO in the respective atmospheres.

Figure 3*a* depicts the two solar temperature profiles: model "0," the non–LTE-blanketed radiative-equilibrium atmosphere of Anderson (1989; his model 2); and model "1," the semiempirical chromosphere-photosphere of Avrett (1985; his model C′). The latter reproduces the spatially averaged emissions of Ca II and other important chromospheric diagnostics. We smoothly joined the high layers of the Anderson model to the Avrett model at the minimum temperature of the latter. The splicing ensures that the continuous energy distributions of the two models will be nearly the same: any differences between synthesized CO spectra will be due primarily to the divergent thermal structures above T_{min} (sharp *drop* in the RE model; sharp *rise* in the semiempirical model).

Figure 3*b* depicts the two analogous models of Arcturus: model "2," similar to the LTE CO-cooled RE photosphere of Heasley *et al.* (1978), on which we imposed a boundary temperature of 2000 K; and model "3," a semiempirical chromosphere like that proposed by Ayres and Linsky (1975). Again, we joined the outer layers of the RE model smoothly to the photosphere of the semiempirical model. We adopted metal abundances of 0.33 solar (Mäckle *et al.* 1975), and a surface gravity of 50 cm s^{-1} (Ayres and Johnson 1977).

We assumed a broadening velocity of 2 km s^{-1} for the Sun (VAL) and 2.5 km s^{-1} for Arcturus (Ayres and Linsky 1975). We discretized each thermal profile onto a grid of 48 plane-parallel layers spaced to provide adequate optical-depth resolution for the CO bands and the mid-IR continuum.

g) *Non–LTE Simulations*

We conducted a series of numerical simulations for the illustrative thermal models. We solved full non–LTE problems for $^{12}C^{16}O$ and $^{13}C^{16}O$ assuming identical molecular parameters aside from abundance. We included the weak isotopic bands of $^{12}C^{18}O$, but treated them in LTE. For the solar models we

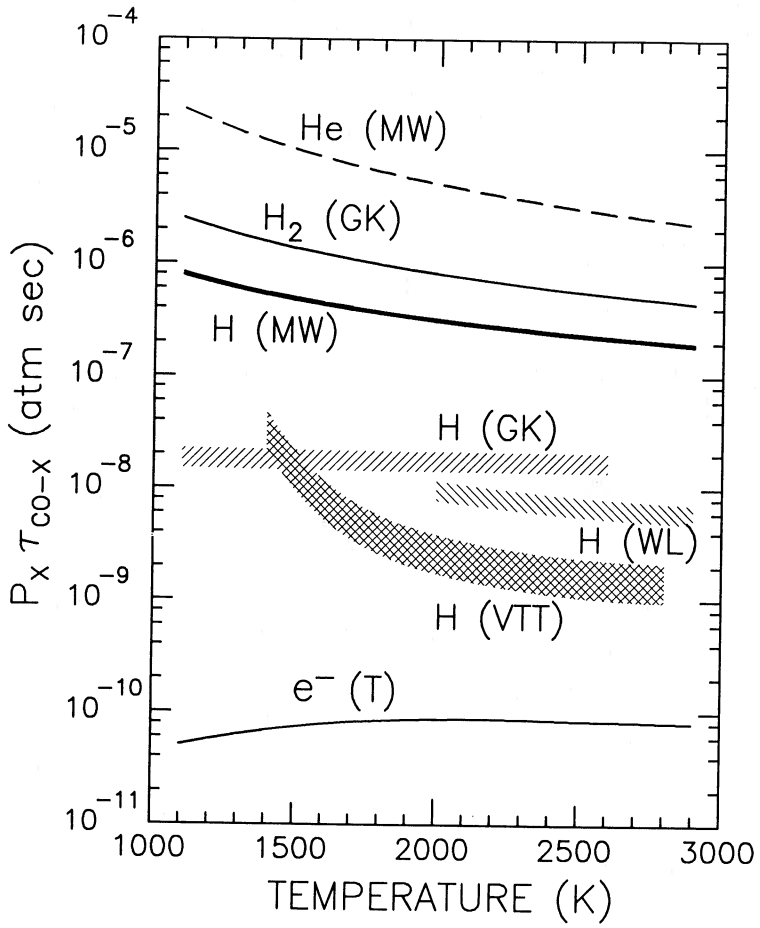

FIG. 2.—Comparison of CO collisional relaxation times for a variety of collision partners. Directly measured values for CO-H are illustrated as hatched bands depicting the ranges of *Pτ*'s allowed by experimental uncertainties. The heavy curve represents the CO-H rate predicted by the scaling law of Millikan and White. Abbreviated references are those of Table 2 and the text: "T" refers to Thompson (1973). The relaxation times decrease approximately inversely with the velocity-dependent collision frequency: the rates for electrons are fastest primarily for this reason. However, the interaction cross sections for CO-H greatly exceed those of the relatively inert perturbers like He and H_2, most likely because of the formation of temporary chemical complexes—such as HCO—during the collisions. We adopted the Glass-Kironde (GK) CO-H relaxation times for the non–LTE simulations.

assumed isotopic abundance ratios of $^{12}C/^{13}C = 90$ and $^{16}O/^{18}O = 500$ (solar-system values; Audouze 1977). For the Arcturus models we assumed $^{12}C/^{13}C = 8$ (e.g., Day, Lambert, and Sneden 1973; Hinkle, Lambert, and Snell 1976) and $^{16}O/^{18}O = 500$ (the terrestrial value). Although an early low-resolution study of the CO $\Delta v = 1$ bands in α Boo by Geballe, Wollman, and Rank (1972) suggested $^{16}O/^{18}O \approx 40$, subsequent work by Geballe *et al.* (1977) on other red giants having low ratios of $^{12}C/^{13}C$ like Arcturus found no evidence for $^{16}O/^{18}O$ significantly different from terrestrial.

Figures 4*a*–4*d* illustrate the calculated ϵ's and departure coefficients ($^{12}C^{16}O$ only) for the solar and stellar models. Figures 4*a* and 4*b* demonstrate that the ϵ's for both solar models exceed 10^2 at radial optical depth unity in strong CO transitions. Owing to the large ϵ's, the departures from LTE are quite small in both of the solar models, even in the lowest density layers. Two effects are worth noting, however. First, the ground vibrational level exhibits a departure which is opposite to that of virtually all of the excited levels. Second, the highest excited states in the cool surface layers of the solar RE model ("0") exhibit a reversal in the sense of their departure coefficients: $b_v > b_{v-1}$ for $v = 6, \ldots, 9$. In the hot chromospheric model, on the other hand, the departure coefficients decrease monotonically with increasing v. These effects can be understood as follows.

The ratio of the departure coefficient of level v to that of the next lower level can be rewritten:

$$\Theta_v = 1 - \frac{(1 - \mathcal{J}_v/\mathcal{B})}{\tilde{\epsilon}_v}, \tag{21}$$

where

$$\tilde{\epsilon}_v \equiv 1 + \mathcal{J}_v/c_1 + \epsilon_v . \tag{22}$$

The second term on the right-hand of equation (22) is positive-definite and of order unity, consequently $\tilde{\epsilon}_v \approx \max[1, \epsilon_v]$. When the collisional rates are small, the departure-coefficient ratio is controlled solely by the radiation field ($\mathcal{J}/\mathcal{B}$). When the collsion rates are large, any departures of $\mathcal{J}$ from $\mathcal{B}$ are diluted in proportion to $\tilde{\epsilon}_v \approx \epsilon_v$. Now, the J-state-weighted mean intensity $\mathcal{J}_v$ is characteristic of the thermal radiation emitted in the layers in which the strong rotational lines of the $v' = v$ band form. In higher *optically thin* layers,

$$\mathcal{J}_v(\bar{\tau} \ll 1) \approx \varpi\mathcal{B}(\bar{\tau} \approx 1), \tag{23}$$

where $\bar{\tau}$ is a state-weighted mean optical depth for the band

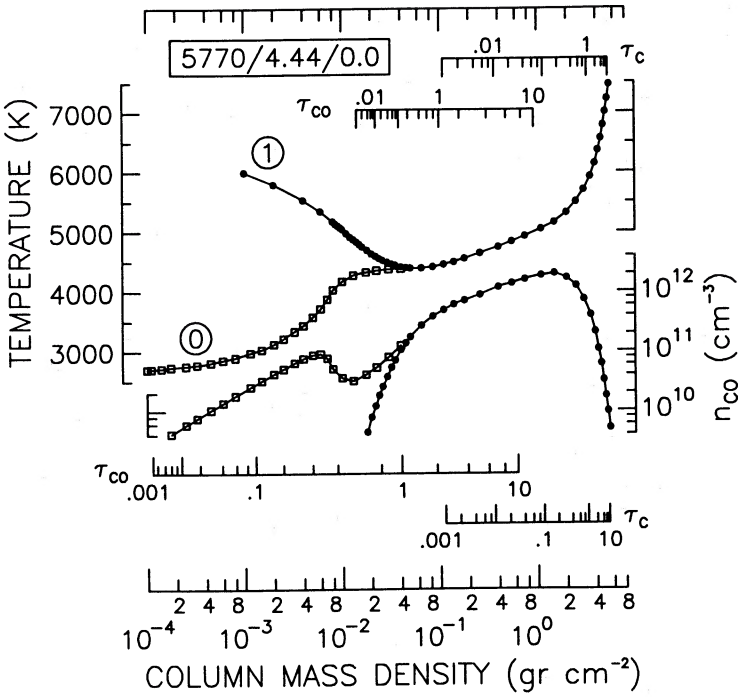

FIG. 3*a*

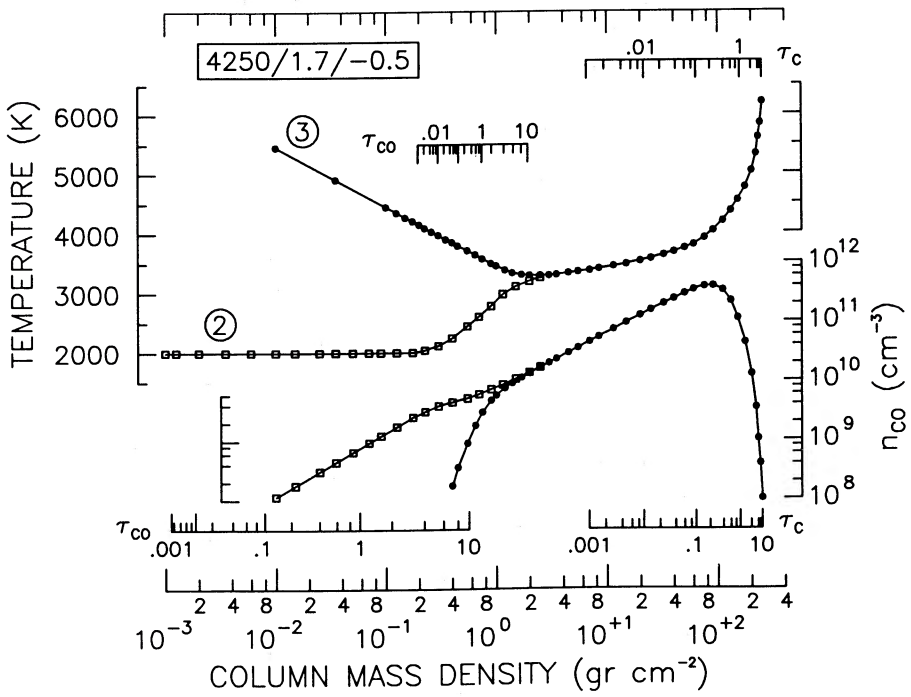

FIG. 3*b*

FIG. 3.—(*a*) Representative models of the solar atmosphere. The box in the upper left corner indicates: T_{eff}, log g, log ($Fe_*/Fe_\odot$). The upper two curves—labeled "0" and "1"—are the thermal profiles: the run of temperature (*left ordinate*) with column mass; the lower two curves are the associated number densities of CO (*right ordinate*). Model 0 (*open squares*) is derived from the non–LTE line-blanketed radiative-equilibrium stratification of Anderson (1989). Model 1 (*dots*) is the semiempirical chromosphere-photosphere described by Avrett (1985). We joined the Anderson model smoothly to the Avrett model at the T_{min} of the latter to ensure identical deep photospheres where the mid-IR continuum forms. Two radial optical depth scales are illustrated for each model: τ_c for the 2100 cm^{-1} continuum; and τ_{CO} for the strong 3–2 R14 line. The optical depth scales for model 0 are in the lower portion of the figure; those for model 1 are in the upper portion. While the continuum optical depth scales are essentially identical, the cool layers of the RE model significantly enhance the CO opacity at small column masses compared to the hot chromospheric model. In the latter the CO has mostly dissociated above T_{min}. (*b*) Same as Fig. 3*a* for representative models of the archetype red giant Arcturus. Note the cooler T_{eff}, substantially reduced surface gravity, and slight metal deficiency of the mild-Population II evolved 1 $M_\odot$ star. Model 2 (*open squares*) is based on the LTE CO-cooled RE model of Heasley *et al.* (1978), on which we have imposed a boundary temperature of 2000 K. Model 3 (*dots*) is the chromospheric thermal structure proposed by Ayres and Linsky (1975) based on a semiempirical study of Ca II. Again, we have spliced the theoretical and semiempirical models at the T_{min} of the latter to ensure identical deep photospheres. Like the solar RE model, the cool outer layers of the RE model of Arcturus substantially raise the altitude at which the strongest CO lines become optically thick. However, unlike the solar chromospheric model, Arcturus model 3 is cool enough to permit the strong CO lines to form above T_{min}: these features should exhibit emission reversals, at least in LTE.

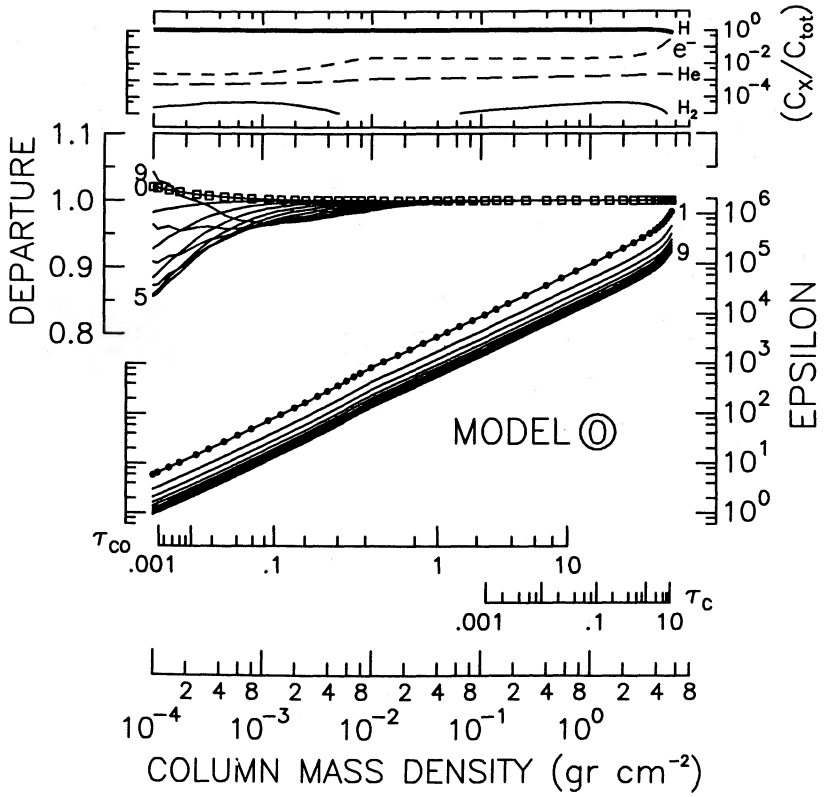

FIG. 4*a*

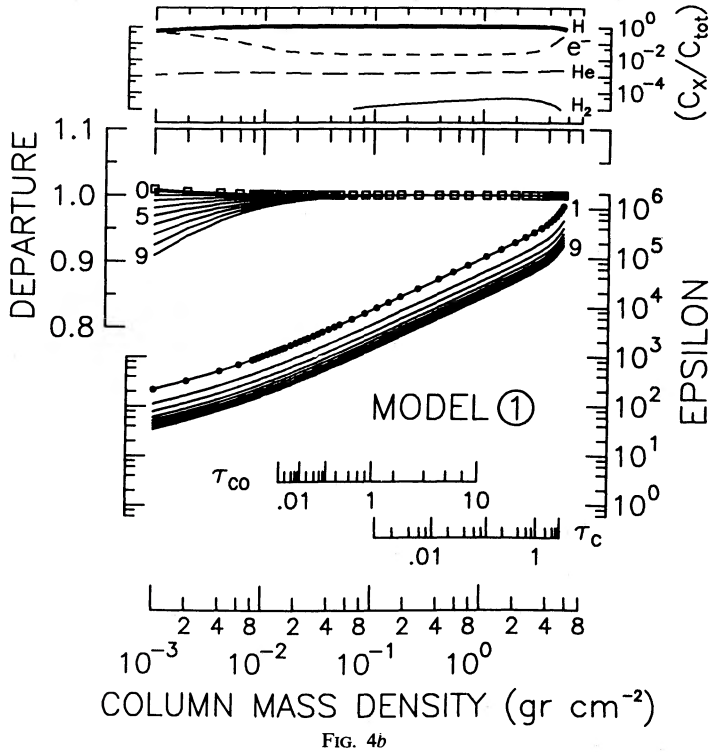

FIG. 4*b*

FIG. 4*a*.—Depth-distributions in solar model 0 of: relative contributions of different collision partners to total de-excitation rate (*upper panel*); collisional ϵ_v's (*right ordinate, main panel*); and associated departure coefficients, b_v, from the non–LTE simulation (*left ordinate, main panel*: $^{12}C^{16}O$ only). The relative contributions to the total collisional rate at each depth are labeled according to the collision partner (*right side of upper panel*): CO-H collsions dominate throughout model 0 owing to the large $T-V$ cross sections and large abundance of atomic hydrogen. The ϵ_v's for the 1–0 vibrational band are depicted by dots and labeled "1" (*right side of main panel*). The ϵ_v's for the remaining bands are indicated by solid curves and decrease monotonically at a fixed column mass with increasing v. The ϵ_v for the 9–8 band is labeled "9." The derived departure coefficients are marked with open squares for the ground vibrational level (*labeled "0" on left side of main panel*) and solid curves for the other nine levels ($v = 5$ and $v = 9$ are labeled explicitly). Reference radial optical-depth scales for CO and the mid-infrared continuum are provided in the lower portion of the main panel. Even though the strongest CO lines have significant opacity in the outer layers of model 0, the densities there are large enough to prevent more than superficial departures from LTE.

FIG. 4*b*.—Same as Fig. 4*a* for solar model 1. Again, the departures from LTE are small and confined to the optically thin layers of the model.

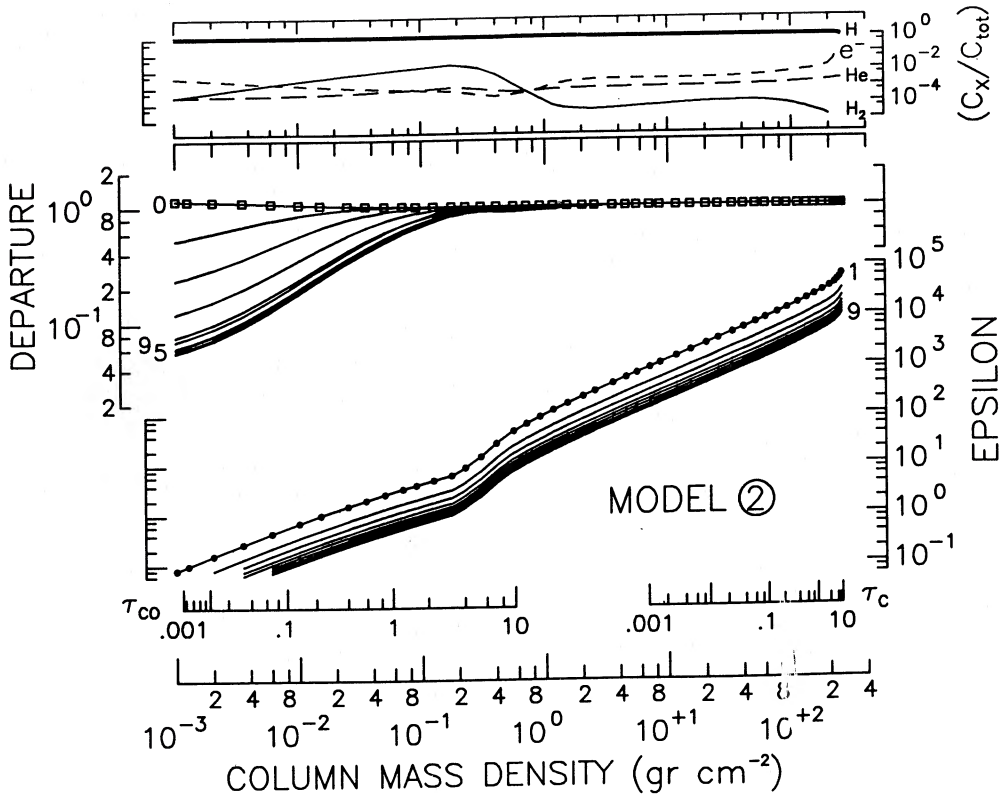

FIG. 4c

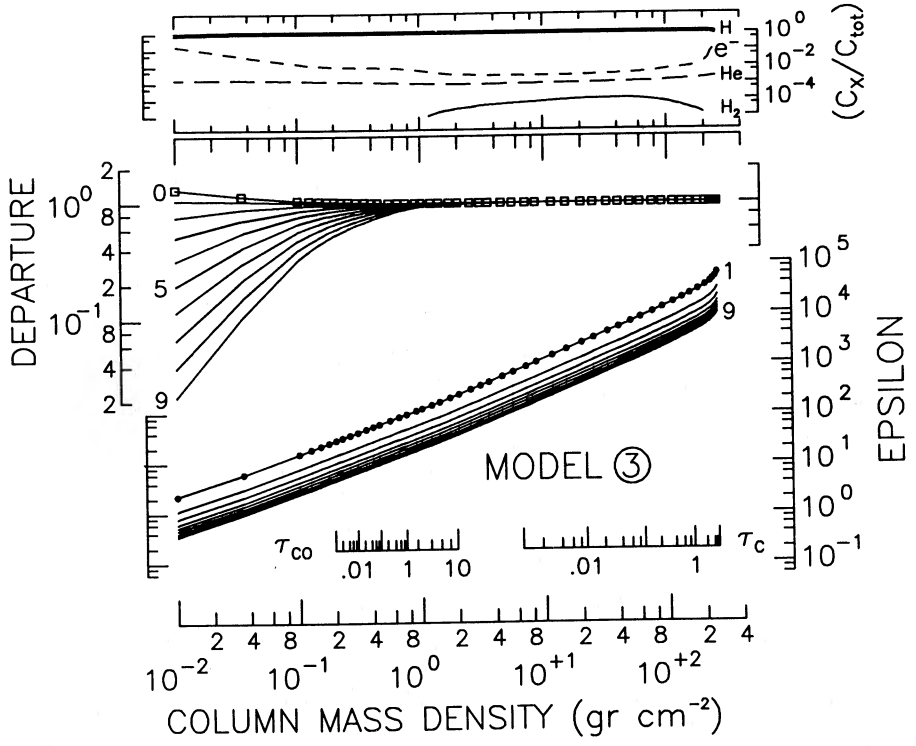

FIG. 4d

FIG. 4c.—Same as Fig. 4a for Arcturus Model 2. The departures from LTE are larger than in the solar models in keeping with the smaller ϵ_v's of the cool tenuous outer layers of the low-gravity RE model. In fact, the departures are nonnegligible where the strong CO lines become thick.

FIG. 4d.—Same as Fig. 4a for Arcturus model 3. The outward rising temperatures of the chromospheric model force the strong CO lines to become thick at larger column masses than in the cool RE model. Although the departures from LTE are larger in the high layers of the chromospheric model, the departures at the depths where the strong CO lines form are smaller than in the RE model.

and ϖ is a dilution factor accounting for the angular average of the local radiation field.

For the strong bands arising from the first few heavily populated vibrational levels, the $\mathscr{J}$'s form relatively high in the atmosphere (near T_{min} in model 1, for example). In the higher optically thin levels of models 0 and 1, the temperatures are, respectively, only somewhat cooler than T_{min} or substantially hotter. Because the mid-IR Planck function is approximately *linear* in temperature, the factor of $\varpi \approx \frac{1}{2}$ in the relation for the mean intensity guarantees that $\mathscr{J} < \mathscr{B}$ for the stronger bands in the superficial layers of both models. Because $\Theta_v < 1$ for at least the first few vibrational levels, they should have successively smaller departure coefficients. On the other hand, the higher vibrational bands arise from the relatively unpopulated excited levels whose $\mathscr{J}$'s are dominated by that of the background continuum. For model 0 the thermal contrast between the superficial layers and the deep photosphere where $\mathscr{J}_C$ forms is sufficient that $\mathscr{J} \gtrsim \mathscr{B}$ in the optically-thin regions. This ensures $\Theta_v \gtrsim 1$ and progressively increasing departure coefficients with increasing v. For model 1 the chromospheric temperatures are comparable to those of the deep photosphere thereby maintaining $\Theta_v < 1$ in the superficial layers. Because most of the excited vibrational levels are *under*populated in the optically thin layers of models 0 and 1, the ground vibrational level ($v = 0$) must be overpopulated to compensate (e.g., eq. [8]): compared to LTE, spontaneous decays exceed absorptions, and population accumulates in $v = 0$ from which no further downward radiative escape is possible. Again—for the solar models at least—these effects are confined to high layers that have essentially no influence on the emergent spectrum.

Figures 4*c* and 4*d* illustrate that the situation for Arcturus is analogous, but the departures from LTE are greater owing to the lower densities prevailing in the outer atmosphere of the red giant. In the cool outer regions of model 2 the ϵ's are only of order unity where the strongest bands become optically thick. However, owing to the hot chromospheric temperatures of model 3, the heights at which the strong CO bands become optically thick are displaced to the deeper denser layers where the ϵ's are $\gtrsim 10$. Thus the departures from LTE in the chromospheric model are smaller *where the* CO *bands form.*

Having calculated departure coefficients for each model we synthesized spectra of the CO bands in a representative interval: 2140–2145 cm^{-1}. We used the simplified energy levels, oscillator strengths, and populations of the non–LTE calculation, but the correct wavenumbers of the transitions to account for the effects of blending. Figure 5 provides a map of

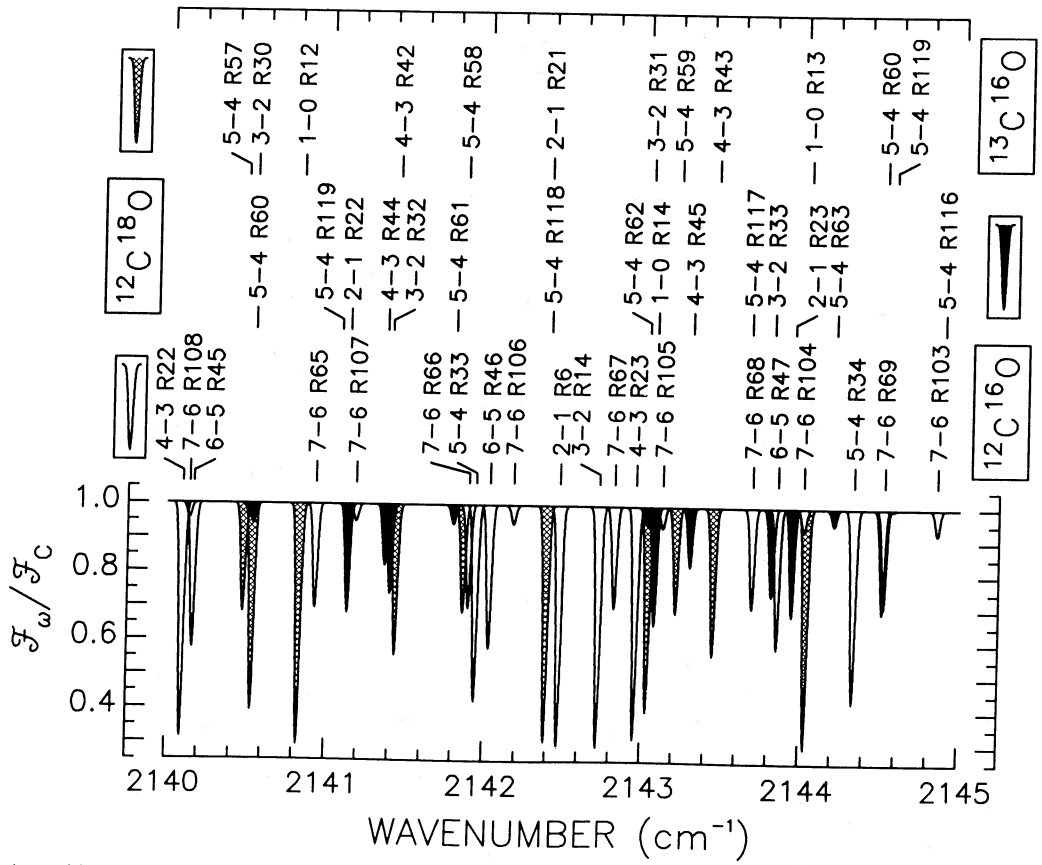

FIG. 5.—CO $\Delta v = 1$ transitions occur throughout a broad region, 1900–2200 cm^{-1}, of the mid-IR. Here we focus on the interval 2140–2145 cm^{-1} (4.67 μm) which has become popular in narrow-band observational studies of the fundamental bands (Geballe, Wollman, and Rank 1972; Wiedemann *et al.* 1987): it is relatively free of contaminating telluric absorptions; it contains strong and weak lines covering a wide range of excitation; and it has contributions from the secondary isotopic bands in addition to $^{12}C^{16}O$. We illustrate an LTE spectrum for that interval synthesized with the RE model of Arcturus. The vibration-rotation lines were calculated independently—not allowing for the blending that occurs in practice—to illustrate their relative contributions. The isotopes and vibration-rotation designations are listed in the upper panel. The secondary isotopic bands were shaded according to the legends there. The $^{12}C^{16}O$ transitions were assigned unfilled profiles that dominate over the other shades. Occasionally a principal line occults an isotopic line of similar strength: e.g., near 2144.5 cm^{-1}. In a comparable synthesis for the Sun, the secondary isotopic bands would be much weaker.

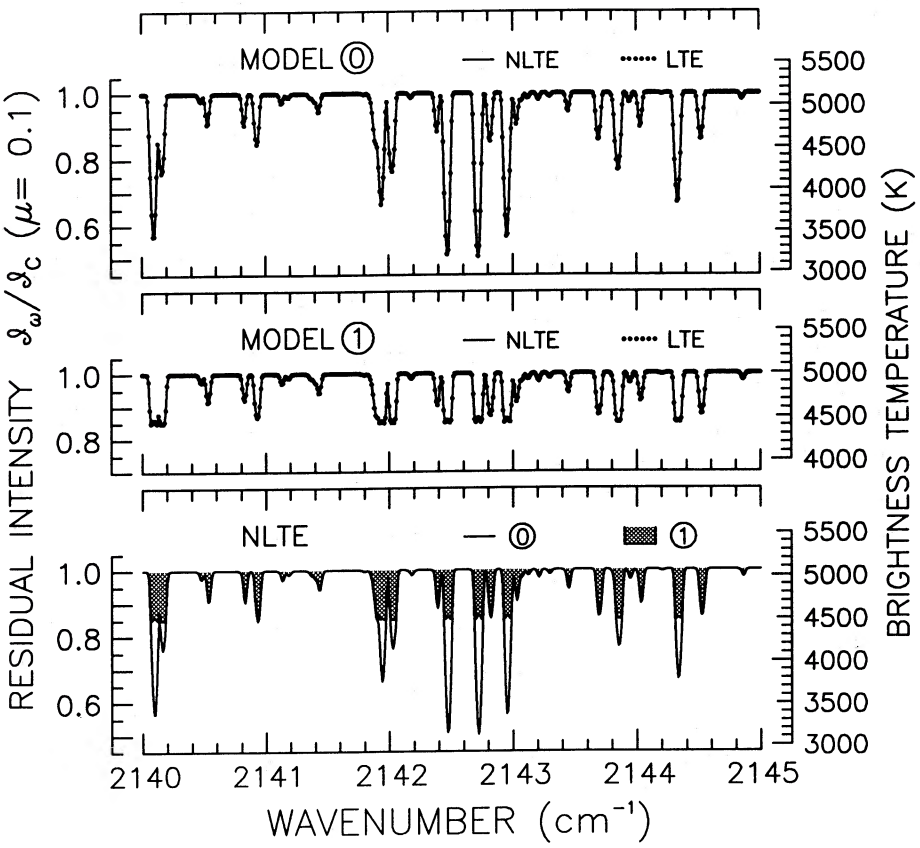

FIG. 6*a*

FIG. 6.—(*a*) CO $\Delta v = 1$ extreme-limb ($\mu = 0.1$) specific intensity spectra for the interval 2140–2145 cm^{-1} synthesized with solar models 0 and 1 under the assumption of LTE and with a full non–LTE treatment. The extreme-limb viewing angle should emphasize any departures from LTE, since the optical depths of the CO lines are amplified relative to the radial column mass density scale by the slant-angle factor μ^{-1}. The upper two panels compare non–LTE and LTE spectra for models 0 and 1 separately; the lower panel compares non–LTE spectra of the two models together. The left-hand ordinate indicates residual intensities; the right-hand ordinate indicates brightness temperatures corresponding to the calculated absolute specific intensities. At the resolution of the diagrams the non–LTE and LTE spectra are identical. However, the differences imposed by the distinct thermal structures of the two models are quite profound. Note the weak emission cores in the extreme-limb spectra of the chromospheric model, while the RE model produces deep absorptions. In both cases the cores of the strong features have saturated to the kinetic temperature near $\tau_{lc}(\mu) \approx 1$. That temperature is high in the chromospheric model ($T_{min} = 4400$ K), and low in the RE model (≈ 3200 K for the extreme-limb viewing angle). Observed limb spectra of the solar CO bands display low brightness temperatures ($\lesssim 3800$ K; $\mu = 0.2$) and no hint of emission reversals. (*b*) Same as (*a*) for flux spectra of the two Arcturus models. While non–LTE and LTE spectra for the chromospheric model 3 are essentially identical, the non–LTE absorption cores of strong CO features are slightly deeper than their LTE counterparts in the spectrum of the RE model 2. The non–LTE core darkening corresponds to, at most, 200 K in brightness temperature. An *underestimate* of the kinetic temperature in the line-forming region of that magnitude would occur in an LTE interpretation: not a serious error in view of the rather dramatic differences between the spectra of the RE and chromospheric models. (Note the pronounced emission cores predicted by the later.) Like the Sun, empirical spectra of the CO $\Delta v = 1$ bands of Arcturus exhibit cool cores similar to those of the RE model.

the principal and secondary isotropic bands of CO in the 5 cm^{-1} interval.

Figure 6*a* depicts synthetic specific intensity spectra for the two solar models at an extreme-limb viewing angle ($\mu = 0.1$). The limb spectrum forms at greater heights than the disk-center intensities and should be more sensitive to subtle density-dependent non–LTE effects. Nevertheless, the non–LTE and LTE spectra are essentially identical. The gross differences produced by the divergent thermal structures of Models 0 and 1 are quite apparent, however. Empirical limb spectra of the solar $\Delta v = 1$ bands are much closer to those of model 0 than model 1 (AT; ATB).

Figure 6*b* illustrates synthetic flux spectra for the two models of Arcturus. One sees a slight deepening—and sharpening—of the non–LTE cores relative to the LTE profiles of the strongest CO features in the RE model 2. In contrast, the non–LTE and LTE spectra are essentially identical for the chromospheric model 3. Again, the spectra predicted by the divergent thermal structures are profoundly different: indeed, the strongest CO features exhibit pronounced emission reversals in the synthetic chromospheric spectrum (see also Heasley and Milkey 1976). As in the solar case, the observed CO spectrum of Arcturus is closer to that of the RE model (Heasley *et al.* 1978).

III. DISCUSSION

It is paradoxical that we encounter the largest differences between non–LTE and LTE spectra in the classical *radiative-equilibrium* model (of Arcturus), while essentially no differences between non–LTE and LTE spectra occur for the highly non-classical thermal structure of the *chromospheric* model. One might have hoped that simple departures from LTE in the chromospheric model would darken the CO line cores and thereby reconcile the recorded pure absorption features with

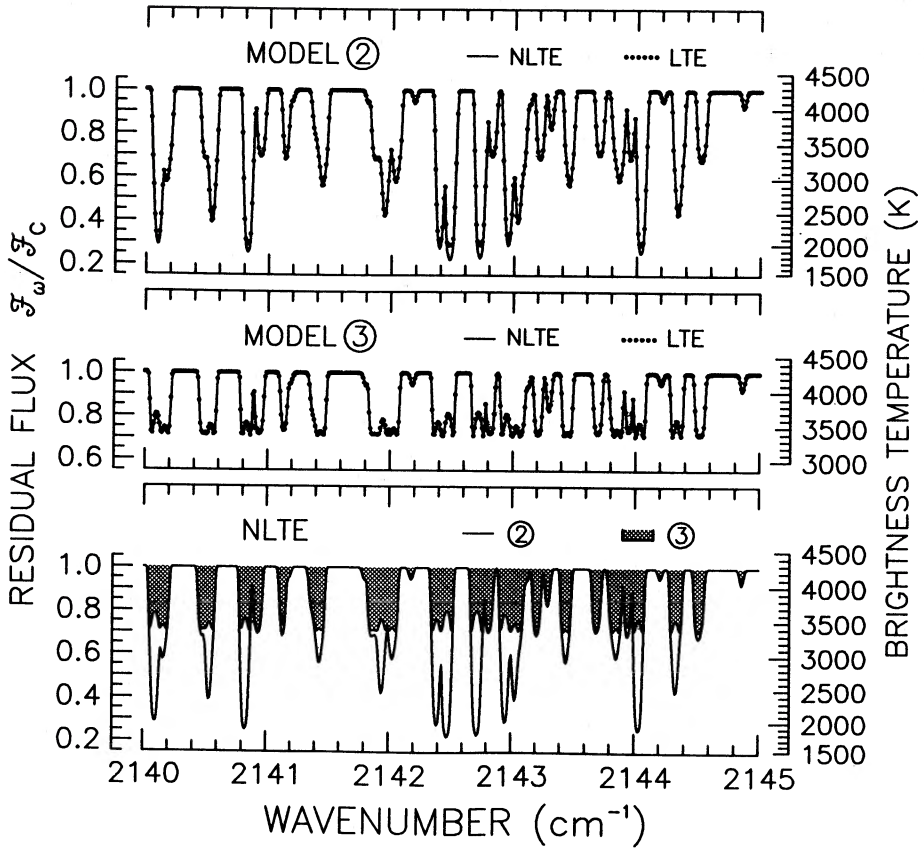

FIG. 6*b*

the presence of the temperature inversion deduced from other diagnostics. Our simulations, however, demonstrate just the opposite: the hot temperatures of the chromospheric model prevent the CO bands from becoming optically thick in the higher tenuous layers where the CO-H collision rates are small and the departures from LTE are large. Thus, the striking empirical dichotomy between the cool cores of the CO bands and the chromospheric emission reversals of species like Ca II must be explained by something other than non–LTE effects on the molecular side.

The departures from LTE are small enough—even in the low-density case of the red-giant RE model—that the LTE assumption should be satisfactory for a wide variety of stars in the cool half of the H-R diagram, particularly F-K dwarfs and subgiants. Specifically, our simulations vindicate the previous LTE interpretations of limb spectra of the solar $\Delta v = 1$ bands.

The major uncertainty in the present work is the detailed behavior of cross sections for H atoms colliding with vibrationally excited CO. We have taken the conservative view that the cross sections are independent of vibrational quantum number. Nevertheless, it is possible that the collisional cross sections *decrease* with increasing v: in that event the departures from LTE will be larger than found in the present work, particularly for the moderately well populated $v = 2$, 3, and 4 levels. Until state-resolved $\Delta v = 1$ relaxation rates are measured in the laboratory, the detailed influence of non–LTE effects on the CO bands of red giants will remain somewhat uncertain. However, the v-dependence would have to be rather pathological to permit any serious departures from LTE in high-gravity dwarf stars like the Sun.

IV. CLOSING REMARKS

We have tackled a formidable non–LTE problem in a complex molecule with many interlocking transitions only to find negligible departures from LTE in situations of practical interest. Some might view our efforts as disappointing, when compared with the spectacular non–LTE effects found in other species.

On the contrary: the ideal spectral diagnostic is one whose excitation is purely in LTE, for it will carry the most faithful mapping of the atmospheric temperatures over which it forms. Our simulations demonstrate that the CO $\Delta v = 1$ bands of late-type atmospheres are close to that LTE ideal. Newly developed cryogenic spectrometers and panoramic IR imagers should permit the great diagnostic promise of the CO "thermometer" to be realized in an even wider range of cosmic problems.

Support for this study was provided by the National Science Foundation through grant AST-8507029 to the University of Colorado, and by the National Aeronautics and Space Administration through grant NGL 06-003-057. We thank J. L. Linsky for his comments on an earlier version of the manuscript.

APPENDIX

TRANSLATIONAL-TO-VIBRATIONAL ENERGY EXCHANGE IN COLLISIONS OF CARBON MONOXIDE WITH ATOMS, DIATOMS, AND ELECTRONS

I. ATOMIC HYDROGEN

HL and CMH employed CO-H cross sections from the work of MW and VTT. MW applied the Landau-Teller formalism to experimental results for a number of relatively inert perturbers like He, Ne, and H_2, and extrapolated the derived parameters to atomic hydrogen. VTT conducted the first direct measurements: a supersonic nozzle-flow experiment for the collisional de-excitation of CO through argon and various diatomic molecules in the presence of small amounts of atomic hydrogen. Fast relaxation times indicated that H atoms are far more efficient collision partners for CO than predicted by the simple scaling laws.

VTT expressed their results in terms of a temperature-dependent 1–0 de-excitation probability (per collision), $\mathscr{P}_{10}$. It is related to the relaxation time as follows:

$$\mathscr{P}_{10} = [t_{\text{CO-H}} Z_{\text{CO-H}} n_{\text{H}}(1 - e^{-\beta})]^{-1} ,$$

where $Z_{\text{CO-H}} = 3 \times 10^{-11} T^{1/2}$ ($\text{cm}^3\ \text{s}^{-1}$) is the collision frequency (based on a velocity-independent cross section of $2 \times 10^{-15}\ \text{cm}^2$ derived from the application of Lennard-Jones [6–12] potentials by Hirschfelder, Curtiss, and Bird 1954, as cited by Glass and Kironde 1982; see also VTT), and n_{H} is the number density of H atoms (cm^{-3}). The de-excitation probabilities reported by VTT range from ~ 0.08 at 2000 K (i.e., eight of 100 collisions results in a 1–0 de-excitation) to 0.3 at 2800 K. We convert the probabilities to relaxation times by rewriting the previous equation:

$$P_{\text{H}} t_{\text{CO-H}} = 2.3 \times 10^{-8} T^{1/2} / [\mathscr{P}_{10}(T)(1 - e^{-\beta})] .$$

Relaxation times derived from the VTT de-excitation probabilities are a factor of 10^2 faster than those of MW near 3000 K (a smaller difference than the factor of $\approx 10^3$ indicated in Fig. 1 of HL and CMH). While still not completely satisfactory, the understanding of translational-to-vibrational (T–V) energy exchange in CO-H has improved in recent years.

First, Glass and Kironde (1982, hereafter GK) measured CO-H relaxation times in a shock-tube experiment where trace amounts of atomic hydrogen and CO were buffered by argon and an admixture of molecular hydrogen. The authors describe their results by Landau-Teller parameters of $A = 3 \pm 2$ and $B = 18.1 \pm 0.2$. The GK P t's are similar to the VTT values at 1500 K, but an order of magnitude slower at 2600 K ($\mathscr{P}_{10}{}^{\text{GK}} \approx 0.017$ vs. $\mathscr{P}_{10}{}^{\text{VTT}} \approx 0.2$). Near 3000 K the (extrapolated) GK de-excitation rates fall logarithmically midway between those of MW and VTT.

Second, Wight and Leone (1983, hereafter WL) measured the absolute probability for T–V excitation of CO by hot atomic hydrogen in a molecular beam experiment that incorporated a novel excimer laser photolysis technique. Although the high kinetic energy ($\gtrsim 0.95$ eV $\approx 10^4$ K) of the H atoms in the authors' experiment precludes a direct comparison to the VTT and GK relaxation times, we attempted to connect them as follows. WL tabulate a transfer probability $\mathscr{P}(E)$ as a function of the translational energy of the incident H atom. (Note: the WL transfer probability is derived from mono-energetic collisions and thus differs from the *isothermal* transfer probabilities described previously. The latter effectively integrate over the Maxwellian velocity distribution of the collision partners.) We converted to the number of vibrational excitations per H-atom collision, and extrapolated $\mathscr{P}(E)$ to the low-energy cutoff, $E_0 \approx \omega_0$. We then integrated the probability function over a Maxwellian velocity distribution incorporating the velocity-independent interaction cross section described previously. Finally, we estimated the associated relaxation times by applying the inverse of equation (19). The inferred rates are 2–3 times faster than the GK values in the temperature range 2000–3000 K. We consider the agreement good in view of the uncertainties: the derived relaxation times depend sensitively on the extrapolation of $\mathscr{P}(E)$ to lower energies, particularly near the cutoff.

We base our non–LTE simulations on the collisional relaxation times proposed by Glass and Kironde because their Landau-Teller parameters are more directly transformed into excitation rates than the discrete-energy interaction probabilities of the Wight-Leone experiment. GK specify their results in terms of the relaxation rate for the $v' = 1$ level. However, the spectral range recorded in the authors' study is "contaminated" by $\Delta v = 1$ emissions from higher v states populated at shock-tube temperatures. Their contribution should be assessed to establish the true de-excitation rate for 1–0. Further, the proper treatment of CO in late-type atmospheres also requires a thorough understanding of the higher $v' \rightarrow (v' - 1)$ collisional transitions.

HL argue that the collisional coefficients for the higher bands scale from Ω_{10} according to the "symmetric-top" model, which predicts $\Omega_{v'v'-1} \sim v'\Omega_{10}$. With such a scaling the collisional coupling parameters $\epsilon_{v'}$ would be nearly *independent* of v' because the band spontaneous decay rates also increase $\sim v'$ (Table 1; HL, their § 3.6). However, if the $\Omega_{v'v'-1}$ are *independent* of v' or *decrease* with increasing v', $\epsilon_{v'}$ will *decrease* systematically with increasing v', implying larger departures from LTE in the higher bands.

Unfortunately, we have not found any experimental data for cross sections of H atoms colliding with CO in excited v levels of its ground electronic state. Nevertheless, a few studies are peripherally relevant:

1. The results of GK (and WL) strongly suggest that the formation of temporary chemical complexes (e.g., HCO) dominates the relaxation process, and rule out the strongly v-dependent SSH mechanism (Schwartz, Slawsky, and Herzfeld 1952). The latter is important for the relaxation of CO through self-collisions or collisions with other diatomic molecules (e.g., Bray 1968). The *shortening* of relaxation times with increasing v mentioned by VTT as an extension of the SSH process therefore does not apply to the excitation of CO in a stellar atmosphere where collisions with hydrogen atoms are orders of magnitude more efficient and frequent than collisions with molecules.

2. The collisional quenching of $v > 0$ states in *electronically excited* CO was investigated by Fink and Comes (1974). CO molecules were selectively pumped into different vibrational levels of $A^1\Pi$ in the presence of nobel gases. Examination of the fluorescence spectra yielded effective cross sections for the vibrational relaxation of those states. The results for Ar and Kr—which

potentially can form weak complexes with CO—are of particular interest. They suggest that the $\Delta v = 1$ de-excitation efficiency decreases slowly, if at all, with increasing vibrational quantum number. However, extrapolations to the electronic ground state and to the highly reactive CO-H system are uncertain.

3. A *slowing* of relaxation times with increasing v is seen in other systems (not including H as a collision partner) apparently involving a variety of mechanisms: a discussion of these is provided by Procaccia and Levine (1975). Again, the relevance to CO-H collisions is uncertain.

In the absence of clear experimental or theoretical guidance, we assume that the collisional de-excitation rates for CO-H (and CO-*X* in general) are *independent* of the initial vibrational quantum state.

II. MOLECULAR HYDROGEN

We also adopted the Glass and Kironde result for molecular hydrogen: the GK Landau-Teller parameters are nearly identical to those of Hooker and Millikan (1963). The Hooker-Millikan relaxation times, in turn, have been substantiated by the theoretical work of Stricker (1978), among others. In our stellar models the number density of molecular hydrogen usually is considerably smaller than that of atomic hydrogen: this and the reduced T–V cross section guarantee that CO-H_2 is not a significant collisional process.

III. HELIUM

We adopted Millikan's (1964) result for helium: it has been corroborated by the experimental/theoretical study of Maricq *et al.* (1983) and by the theoretical work of Schinke and Diercksen (1985), among others. However, like CO-H_2, CO-He is not a significant collisional process in our stellar models.

IV. ELECTRONS

We adopted Thompson's (1973) schematic cross sections for electron collisions. At low temperatures the de-excitation rate coefficient is

$$\Omega_{10} \approx 1.4 \times 10^{-9}\beta^{-1/2}[(1+\beta) + 19e^{-3.22\beta}(1+4.22\beta)] .$$

The electron collisional rates are significant only where $n_e/n_H \gtrsim 10^{-2}$. Because the abundance of CO is negligible in such layers, CO-e^- also is not an important factor in the non–LTE problem.

REFERENCES

Allen, C. W. 1973, *Astrophysical Quantities* (3d ed.; London: Athlone).
Anderson, L. S. 1989, *Ap. J.*, in press.
Audouze, J. 1977, in *CNO Isotopes in Astrophysics*, ed. J. Audouze (Dordrecht: Reidel), p. 3.
Auer, L. H. 1976, *J. Quant. Spectrosc. Rad. Transf.*, **16**, 931.
Auer, L. H., and Heasley, J. N. 1976, *Ap. J.*, **205**, 165.
Auer, L. H., Heasley, J. N., and Milkey, R. W. 1972, *KPNO Contrib.*, No. 555.
Avrett, E. H. 1985, in *Chromospheric Diagnostics and Modeling*, ed. B. Lites (Sunspot, NM: National Solar Observatory), p. 67.
Ayres, T. R. 1979, *Ap. J.*, **228**, 509.
———. 1981, *Ap. J.*, **244**, 1064.
Ayres, T. R., and Johnson, H. R. 1977, *Ap. J.*, **214**, 410.
Ayres, T. R., and Linsky, J. L. 1975, *Ap. J.*, **200**, 660.
Ayres, T. R., and Testerman, L. 1981, *Ap. J.*, **245**, 1124 (AT).
Ayres, T. R., Testerman, L., and Brault, J. W. 1986, *Ap. J.*, **304**, 542 (ATB).
Bray, K. N. C. 1968, *J. Phys. B*, **1**, 705.
Carbon, D. F., Milkey, R. W., and Heasley, J. N. 1976, *Ap. J.*, **207**, 253 (CMH).
Day, R. W., Lambert, D. L., and Sneden, C. 1973, *Ap. J.*, **185**, 213.
Fink, E. H., and Comes, F. J. 1974, *Chem. Phys. Letters*, **25**, 2.
Foing, B., and Bonnet, R. M. 1984, *Ap. J.*, **279**, 848.
Geballe, T. R., Wollman, E. R., Lacy, J. H., and Rank, D. M. 1977, *Pub. A.S.P.*, **89**, 840.
Geballe, T. R., Wollman, E. R., and Rank, D. M. 1972, *Ap. J. (Letters)*, **177**, L27.
Glass, G. P., and Kironde, S. 1982, *J. Phys. Chem.*, **86**, 908 (GK).
Hall, D. N. B. 1970, Ph.D. thesis, Harvard University.
Heasley, J. N., and Milkey, R. W. 1976, *Ap. J. (Letters)*, **205**, L43.
Heasley, J. N., Ridgway, S. T., Carbon, D. F., Milkey, R. W., and Hall, D. N. B. 1978, *Ap. J.*, **219**, 790.
Hinkle, K. H., and Lambert, D. L. 1975, *M.N.R.A.S.*, **170**, 447 (HL).
Hinkle, K. H., Lambert, D. L., and Snell, R. L. 1976, *Ap. J.*, **210**, 684.
Hirschfelder, J. O., Curtiss, C. F., and Bird, R. B. 1954, *Molecular Theory of Gases and Liquids* (New York: Wiley).
Hooker, W. J., and Millikan, R. C. 1963, *J. Chem. Phys.*, **38**, 214.
Johnson, H. R. 1973, *Ap. J.*, **180**, 81.
Kirby-Docken, K., and Liu, B. 1978, *Ap. J. Suppl.*, **36**, 359.
Kurucz, R. L. 1970, *SAO Spec. Rept.*, No. 309.
———. 1976, *SAO Spec. Rept.*, No. 374.
Mäckle, R., Griffin, R., Griffin, R., and Holweger, H. 1975, *Astr. Ap.*, **38**, 239.
Mantz, A. W., Maillard, J.-P., Roh, W. B., and Rao, K. N. 1975, *J. Molec. Spectrosc.*, **57**, 155.
Maricq, M. M., Gregory, E. A., Wickham-Jones, C. T., Cartwright, D. J., and Simpson, C. J. S. M. 1983, *Chem. Phys.*, **75**, 347.
Mihalas, D. 1978, *Stellar Atmospheres* (2d ed.; San Francisco: Freeman).
Millikan, R. C. 1964, *J. Chem. Phys.*, **40**, 2594.
Millikan, R. C., and White, D. R. 1963, *J. Chem. Phys.*, **39**, 3209 (MW).
Noyes, R. W., and Hall, D. N. B. 1972, *Ap. J. (Letters)*, **176**, L89.
Procaccia, I., and Levine, R. D. 1975, *J. Chem. Phys.*, **63**, 4261.
Radzig, A. A., and Smirnov, B. M. 1985, *Reference Data on Atoms, Molecules, and Ions* (New York: Springer-Verlag).
Schinke, R., and Diercksen, G. H. F. 1985, *J. Chem. Phys.*, **83**, 4516.
Schwartz, R. N., Slawsky, Z. I., and Herzfeld, K. F. 1952, *J. Chem. Phys.*, **20**, 1591.
Stricker, J. 1978, *J. Chem. Phys.*, **68**, 934.
Thompson, R. I. 1973, *Ap. J.*, **181**, 1039 (T).
Vernazza, J. E., Avrett, E. H., and Loeser, R. 1973, *Ap. J.*, **184**, 605 (VAL).
———. 1976, *Ap. J. Suppl.*, **30**, 1.
———. 1981, *Ap. J. Suppl.*, **45**, 635.
von Rosenberg, C. W., Jr., Taylor, R. L., and Teare, J. R. 1971, *J. Chem. Phys.*, **54**, 1974 (VTT).
Wiedemann, G., Ayres, T., Jennings, D., and Saar, S. 1987, in *Cool Stars, Stellar Systems, and the Sun*, ed. J. L. Linsky and R. E. Stencel (New York: Springer-Verlag), p. 374.
Wight, C. A., and Leone, S. R. 1983, *J. Chem. Phys.*, **78**, 4875 (WL).

THOMAS R. AYRES: Center for Astrophysics and Space Astronomy, Campus Box 391, University of Colorado Boulder, CO 80309-0391

GÜNTER R. WIEDEMANN: Goddard Space Flight Center, Code 693, Building 2, Greenbelt, MD 20771